[CANCER RESEARCH 61, 8179–8187, November 15, 2001]

Quantitative Imaging and Microlocalization of Boron-10 in Brain Tumors and Infiltrating Tumor Cells by SIMS Ion Microscopy: Relevance to Neutron Capture Therapy[1]

Duane R. Smith[2], Subhash Chandra, Rolf F. Barth, Weilian Yang, Darrel D. Joel, and Jeffrey A. Coderre[3]

Department of Chemistry and Chemical Biology, Cornell University, Ithaca, New York 14853 [D. R. S., S. C.]; Department of Pathology, The Ohio State University, Columbus, Ohio 43210 [R. F. B., W. Y.]; and Medical Department, Brookhaven National Laboratory, Upton, New York 11973 [D. D. J., J. A. C.]

ABSTRACT

Boron neutron capture therapy (BNCT) is dependent on the selective accumulation of boron-10 in tumor cells relative to the contiguous normal cells. Ion microscopy was used to evaluate the microdistribution of boron-10 from *p*-boronophenylalanine (BPA) in the 9L rat gliosarcoma and the F98 rat glioma brain tumor models. Four routes of BPA administration were used: i.p. injection, intracarotid (i.c.) injection [with and without blood-brain barrier disruption (BBB-D)], and continuous timed i.v. infusions. i.p. injection of BPA in the 9L gliosarcoma resulted in a tumor-to-brain (T:Br) boron-10 concentration ratio of 3.7:1 when measured at the tumor-normal brain interface. In the F98 glioma, i.c injection of BPA resulted in a T:Br ratio of 2.9:1, and this increased to 5.4:1 when BBB-D was performed. The increased tumor boron uptake would potentially enhance the therapeutic ratio of BNCT by >25%. At present, ion microscopy is the only technique to provide a direct measurement of the T:Br boron-10 concentration ratio for tumor cells infiltrating normal brain. In the 9L gliosarcoma, this ratio was 2.9:1 after i.p. administration. In the F98 glioma, i.c injection resulted in a ratio of 2.2:1, and this increased to 3.0:1 after BBB-D. Ion microscopy revealed a consistent pattern of boron-10 microdistribution for both rat brain tumor models. The boron-10 concentration in the main tumor mass (MTM) was approximately twice that of the infiltrating tumor cells. One hour after a 2-h i.v. infusion of BPA in rats with the 9L gliosarcoma, tumor boron-10 concentrations were 2.7 times higher than that of infiltrating tumor cells [83 ± 23 μg/g tissue *versus* 31 ± 12 μg/g tissue (mean ± SD)]. Continuous 3- and 6-h i.v. infusions of BPA in the 9L gliosarcoma resulted in similar high boron-10 concentrations in the MTM. The boron-10 concentration in infiltrating tumor cells was two times lower than the MTM after a 3-h infusion. After 6 h, the boron-10 concentration in infiltrating tumor cells had increased nearly 90% relative to the 2- and 3-h infusions. A 24-h i.v. infusion resulted in similar boron-10 levels between the MTM and the infiltrating tumor cells. Boron concentrations in the normal brain were similar for all four infusion times (~20 μg/g tissue). These results are important for BNCT, because clinical protocols using a 2-h infusion have been performed with the assumption that infiltrating tumor cells contain equivalent amounts of boron-10 as the MTM. The results reported here suggest that this is not the case and that a 6-h or longer infusion of BPA may be necessary to raise boron-10 levels in infiltrating tumor cells to that in the MTM.

INTRODUCTION

Clinical trials of BNCT[4] for the treatment of malignant brain tumors and melanoma have recently been carried out or are in progress in the United States, Europe, and Japan (1–4). BNCT is a binary radiotherapeutic modality, which has the potential to selectively irradiate tumor tissue. A prerequisite is the preferential accumulation of ^{10}B in tumor cells, which are then irradiated with low-energy neutrons. Fundamentally, BNCT is based on the fission reaction ($^{10}B + {}^{1}n \rightarrow {}^{11}B \rightarrow {}^{7}Li + {}^{4}He(\alpha) + 2.79$ MeV), where a ^{10}B atom captures a "thermal" neutron ($E_{th} < 0.4$ eV) and spontaneously decays to produce the linear recoiling particles ^{4}He (α particle) and ^{7}Li. The high linear energy transfer radiation produced in the $^{10}B(n,\alpha)^{7}Li$ reaction is short range in tissue (~5 μm for ^{7}Li and ~9 μm for ^{4}He) and can produce nonrepairable (5, 6), sublethal, and potentially lethal damage to DNA. For BNCT to be effective, it has been estimated that tumor cells must be loaded with a minimum of 15–30 μg ^{10}B/g tissue to raise the BNC-related dose to the tumor significantly above the background radiation dose (7, 8), which results from capture reactions with normal tissue ^{1}H and ^{14}N. Therefore, the microlocalization and differential accumulation of ^{10}B are critical factors for the therapeutic outcome of BNCT as well as the dose-limiting response of normal tissues in the irradiated volume.

Extensive preclinical and clinical biodistribution studies are necessary to evaluate the efficacy of a boron delivery agent. These studies can be performed using a number of analytical techniques, which, in general, are based on approaches using atomic spectroscopy, radioanalytical, and imaging methods (9, 10). Many of the analytical approaches, such as prompt γ-ray spectroscopy (11) and atomic emission spectroscopy (12, 13), yield average boron concentrations from gross tissue specimens and, therefore, have limited value for studying the microdistribution of boron delivery agents. However, the SIMS-based technique of ion microscopy (14) is particularly well suited for boron microlocalization studies and, as such, is recognized as an essential tool in BNCT (9, 10, 15–17). For >20 years, ion microscopy has been used for bioanalytical studies of elemental and isotopic gradients as well as the subcellular localization of isotopically labeled molecules (17, 18). The ion microscope is a double-focusing magnetic sector-dynamic secondary ion mass spectrometer (17), which maintains the spatial integrity of an analyte sputtered from the surface of the sample, producing images of isotopic distributions, which can be related to tissue histology with a resolution comparable with a high-quality light microscope. The analysis of boron by the ion microscope is not affected by elemental speciation (the free or bound chemical form of boron) within the biological matrix (19, 20). This is a distinct advantage over many other techniques, because it is possible to analyze any experimental compound developed for BNCT. Furthermore, the ion microscope is capable of monitoring physiologically relevant species such as ^{39}K, ^{23}Na, ^{24}Mg, and ^{40}Ca along with ^{10}B and/or ^{11}B for the evaluation of pathological effects as well as potential artifacts induced during sample preparation.

In the present study, ion microscopy was used to compare the selective delivery and accumulation of ^{10}B in the 9L rat gliosarcoma

Received 5/29/01; accepted 9/18/01.

The costs of publication of this article were defrayed in part by the payment of page charges. This article must therefore be hereby marked *advertisement* in accordance with 18 U.S.C. Section 1734 solely to indicate this fact.

[1] Supported by United States Department of Energy Grants DE-FG02-ER61138, DE-AC02-76CH000016, and DE-AC02-98CH10886. Presented in part at the Seventh International Symposium on Neutron Capture Therapy, Zürich, Switzerland, September 4–7, 1996 and the Eighth International Symposium on Neutron Capture Therapy, La Jolla, California, September 13–18, 1998.

[2] To whom requests for reprints should be addressed, at Cornell University, Department of Chemistry and Chemical Biology, Ithaca, NY 14853-1301. Phone: (607) 255-3884; Fax: (607) 255-4137; E-mail: ds50@cornell.edu.

[3] Present address: Department of Nuclear Engineering, Massachusetts Institute of Technology, Cambridge, MA 02139.

[4] The abbreviations used are: BNCT, boron neutron capture therapy; BNC, boron neutron capture; SIMS, secondary ion mass spectrometry; BPA, *p*-boronophenylalanine; i.c., intracarotid; BBB-D, blood-brain barrier disruption; T:Br, tumor-to-brain; b.w., body weight; MTM, main tumor mass; CNT, contiguous normal brain tissue; BBB, blood-brain barrier; T:Bl, tumor-to-blood.

and the F98 rat glioma brain tumor models treated with the clinical compound, BPA. Four routes of administration were used: i.p. injection, i.c. injection (without BBB-D), i.c. injection (with BBB-D), and continuous timed i.v. infusions. The objective was to assess the T:Br ^{10}B concentration ratio in regions of the tumor-brain interface and more importantly in areas of the brain exhibiting microscopic tumor infiltration. This ratio is important because the effectiveness of BNCT is related primarily to the selective accumulation of the boron delivery agent in the tumor relative to the contiguous normal tissues. At present, ion microscopy is the only technique that has been used specifically to measure ^{10}B concentrations in infiltrating tumor cells. The observations shown here lead to the calculation of the ^{10}B concentration ratio between regions of tumor cells in the MTM and tumor cells infiltrating the normal brain. This empirical ratio is particularly important for BNCT, because clinical protocols using BPA have, to date, been performed with the assumption that infiltrating tumor cells in the normal brain contain equivalent amounts of ^{10}B as tumor cells composing the MTM. The results of the ion microscopy studies presented here contradict this assumption, and they provide support for longer BPA infusion protocols.

MATERIALS AND METHODS

Materials. BPA (95 atom% ^{10}B, L-isomer) was purchased from Boron Biologicals, Inc. (Raleigh, NC). BPA was administered in solution as a fructose complex, the preparation of which has been described elsewhere (21, 22). Polished high purity N-type semiconductor grade silicon wafers were purchased from Silicon Quest International (Santa Clara, CA). High purity, 99.999%, indium sheets (0.010″ thick × 6″ × 6″) were purchased from Surepure Chemetals, Inc. (Florham Park, NJ).

Rat 9L Gliosarcoma. Male Fischer 344 rats weighing ~250 g had 10^4 9L gliosarcoma cells implanted 5 mm beneath the surface of the skull in the left frontal striatum of the brain, as described previously (23). The 9L gliosarcoma originated from an *N*-nitrosomethylurea-induced neoplasm in a Fischer 344 rat, and the history of this tumor has been described in detail elsewhere (24). Administration of BPA and biodistribution studies were initiated 14 days after implantation when tumors were ~4 mm in diameter (40–50 mg).

For compound delivery via a single i.p. injection, four rats (trial 1) received 1200 mg BPA/kg b.w. Observations from the initial trial 1 were then confirmed in a more extensive trial 2. Eight rats (trial 2) received 600 mg BPA/kg b.w. The rats were anesthetized by single i.p. injection of a mixture of ketamine (140 mg/kg b.w.) and xylazine (28 mg/kg b.w.) and killed 2 h after BPA administration.

The procedure for the i.v. infusion of BPA in rats has been described (25). Briefly, seven rats were anesthetized, and a silastic rubber cannula was inserted into the anterior facial vein with the tip of the cannula secured near the entrance of that vein into the external jugular vein. Continuous timed infusions (2, 3, 6, and 24 h; see Table 2) were initiated after recovery from anesthesia using small animal infusion swivels (Harvard Apparatus, South Natick, MA) with spring tethers and calibrated syringe pumps. The rats were anesthetized by single i.p. injection of a mixture of ketamine (140 mg/kg b.w.) and xylazine (28 mg/kg b.w.) and killed 1 h after BPA administration.

There is a significant problem with the 24-h infusion that should be noted. Because the total blood volume of rats is small, volume overload can be lethal, and a dose rate of 250 mg BPA/kg/h for 24 h was invariably fatal. Only one of two rats survived when the dose rate was reduced to 125 mg BPA/kg/h.

Rat F98 Glioma. The rat F98 glioma (American Type Culture Collection) has been described in detail elsewhere (24, 26), and its biological behavior and lack of response to therapy closely simulate that of human high-grade brain tumors. Male Fischer 344 rats weighing ~200 g were inoculated with 10^5 F98 glioma cells using a stereotactic intracranial implantation procedure described elsewhere (27). BPA administration and tissue sampling were initiated on days 10 and 11 after tumor cell inoculation. Two rats were infused with mannitol via i.c. injection to induce osmotic BBB-D as described previously (28). Two rats were infused with saline as controls. All four of the rats, with and without BBB-D, received 300 mg BPA/kg b.w. via i.c. injection. The rats were anesthetized using halothane and killed 2.5 h after BPA administration. It should be noted that microlocalization studies with ion microscopy can produce enormous amounts of imaging data in cryogenically prepared reliable samples. Therefore, consistent and meaningful observations can be based on multiple image analyses from as little as two animals. Furthermore, consistent patterns of boron microdistributions in multiple animal models, such as those shown in the present study, provides a high level of confidence in the observations.

The animal studies described above were reviewed and approved by the Institutional Animal Care and Use Committee of the Brookhaven National Laboratory and by the Institutional Laboratory Animal Care and Use Committee of The Ohio State University.

Sample Preparation for Ion Microscopy. All of the tissues for ion microscopy analysis were cryogenically prepared. Tissue specimens from rats were plunged in liquid isopentane cooled to −150°C in liquid nitrogen. Tissues were sectioned in a cryostat microtome operated with a chamber temperature of ≤−20°C. Sections, 4-μm thick, were taken in series to correlate histological features (via light microscopy) with ^{10}B and other ion gradients (via ion microscopy). Sections prepared for viewing with a light microscope were placed on clean glass microscope slides and stained with H&E. Those sections prepared for analysis with the ion microscope were mounted on cold (≤−20°C), high-purity indium/silicon substrates (29) transferred from the cryostat chamber on dry ice to a vacuum freeze dryer held at −60°C and freeze-dried for a period of 24 h. Before removal from the vacuum chamber of the freeze dryer, the samples were warmed in stepwise 10°C increments (15 min between steps) to a final temperature of 40°C to avoid rehydration. The tissues were coated with a minimum of 400 Å of Au/Pd alloy before ion microscopy analysis. Freeze-dried specimens, coated or uncoated, were transferred to small plastic dishes and stored in a glass dessicator containing anhydrous calcium sulfate (Drierite).

Ion Microscopy Imaging. A CAMECA IMS-3F ion microscope (Paris, France), a direct-imaging secondary ion mass spectrometer (17), was used in the present studies. The use of this instrument for BNCT related microlocalization studies as well as other bioanalytical/medical applications, has been described previously (15–17). The ion microscope was operated in the positive secondary ion imaging mode with samples biased to +4500 V. An O_2^+ primary ion beam, accelerated to either 10 keV or 12.5 keV, was focused and adjusted to a nominal beam current of 100–140 nA with a diameter of ~50 μm when viewed as a stationary spot at the surface of the sample. In most analyses, the primary ion beam was raster scanned over 250-μm × 250-μm square regions. The rate of erosion of the tissue specimens was ~20 Å/s. Single-charged positive secondary ions, originating from the surface of the sample, were collected as a global (nonmass-filtered) image by the immersion lens of the instrument and focused using the 150-μm transfer optics in conjunction with a 60-μm contrast aperture. When wider fields-of-view were necessary, the 400-μm transfer optics were used. In all of the cases, the energy window of the mass spectrometer was centered and set to a maximum value of 130 eV. Energy and mass-filtered secondary ion images were magnified and projected on a single microchannel plate/phosphor screen image detection assembly. The gain of the microchannel plate was set to 70% of maximum. Images were recorded from the image detection assembly using a Photometrics, Ltd., CH220 charged-coupled device liquid-cooled camera head equipped with a Thomson-CSF TH7882 CDA charged-coupled device camera and digitized to 14 bits/pixel by a Photometrics camera controller. Row and column binning was 2 × 2. For each region of analysis, sequential ion images from ^{39}K, ^{23}Na, ^{10}B, ^{12}C, ^{24}Mg, and ^{40}Ca were acquired using camera integration times of typically 0.2 s, 0.2 s, 2 min, 2 min, 30 s, and 30 s, respectively. At the start of any given study, the sequence of ion images included that from ^{11}B with an integration time of 2 min to confirm the ^{10}B isotope enrichment of BPA. High-mass resolution analyses confirmed that interferences at the studied masses were negligible (30). In control animals not treated with BPA the ^{10}B signal was below the detection limit of the ion microscope (<1 μg/g tissue wet weight).

Image Processing, Boron Quantification, and Statistical Analysis. Digitized images of ion gradients were analyzed using Alice 2.4.0 image processing software for the Macintosh (Hayden Image Processing Group). Assignment of concentration values to ion images was made using an ion microscopy relative sensitivity factor calibration approach for biological specimens (30)

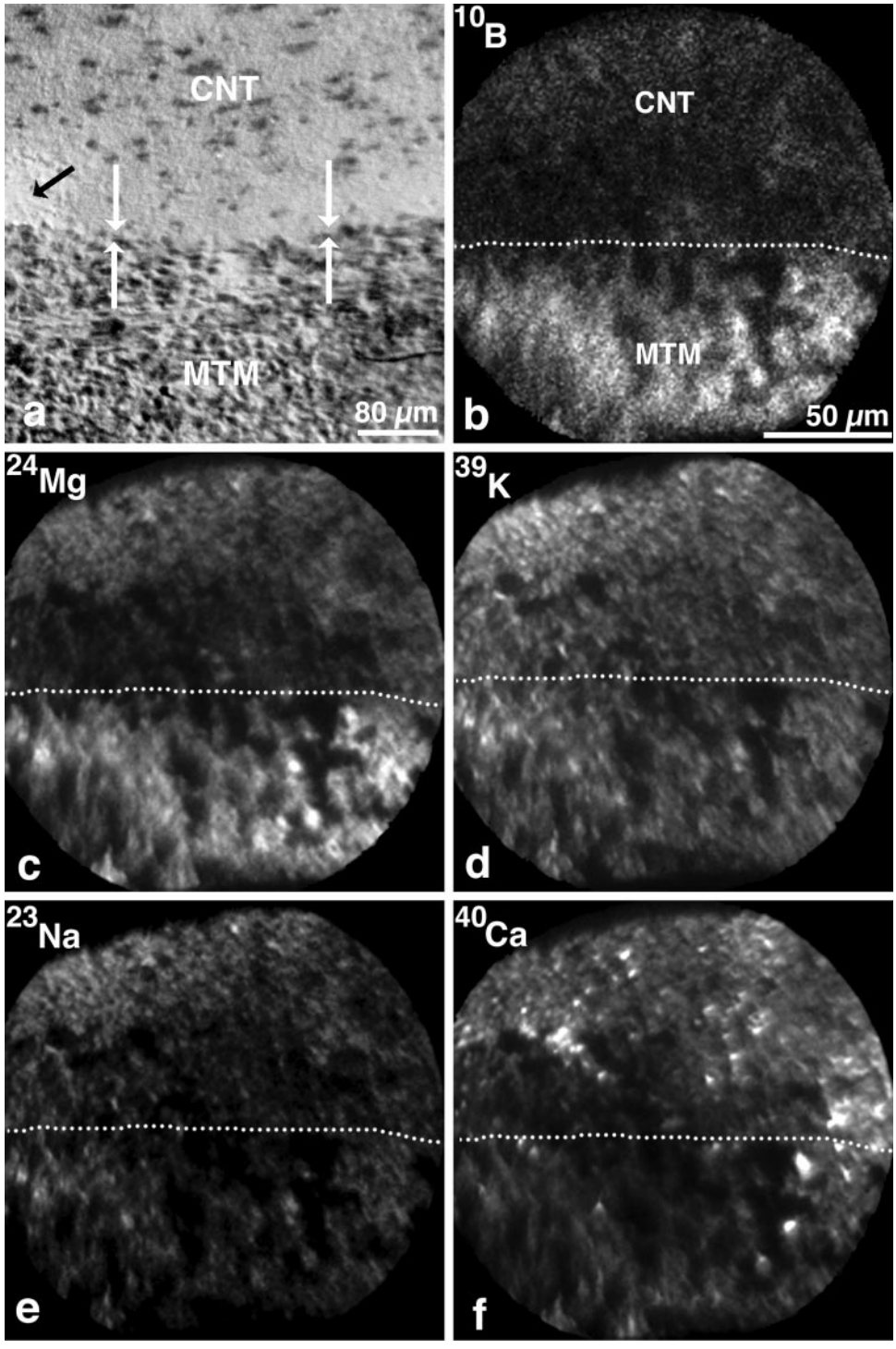

Fig. 1. Interface between the MTM and the normal brain of a male Fischer 344 rat bearing the 9L gliosarcoma. Adjacent 4-μm thick cryosections were used for optical microscopic and ion microscopic imaging. *a*, optical image of a H&E-stained cryosection on glass. *b–f*, ion images from the freeze-dried cryosection showing the distribution of the isotopes ^{10}B (*b*), ^{24}Mg (*c*), ^{39}K (*d*), ^{23}Na (*e*), and ^{40}Ca (*f*) from the same region of analysis. *White arrows* in *a*, interface between a portion of the MTM and the CNT. *Black arrow* in *a*, edematous tissue in the CNT. *Dotted lines* in *b–f*, interface between a portion of the MTM and CNT. Scale for *c–f* is shown in *b*.

which has been used in previous studies[5] (15, 16, 31, 32) for BNCT. Estimates of the ^{10}B concentrations within histological features of interest were determined using the pixel-to-pixel registration and ratio of the ^{10}B and ^{12}C images, the relative sensitivity factor for ^{10}B relative to ^{12}C, and assuming 85% water content. The means and SDs were calculated for concentrations of boron determined from regions within the MTM, clusters of tumor cells infiltrating the normal brain, and the normal brain of the animal models. Tumor:brain and MTM:cluster ^{10}B concentration ratios were calculated as the ratio of the means. The statistical significance of comparable treatments were computed using the ANOVA.

RESULTS

Boron Microlocalization in the Rat 9L Gliosarcoma and the F98 Glioma Brain Tumor Models. Fig. 1*a* shows a representative optical image of a cryosection stained with H&E taken from a rat bearing an intracranial 9L gliosarcoma tumor after i.p. administration of BPA. Arrows indicate a portion of an interface between the MTM and the CNT. The MTM is identified by densely packed, dark-stained nuclei. The cytoplasmic volumes of the tumor cells are small, and

[5] S. Chandra, D. R. Lorey, II, and D. R. Smith. Quantitative subcellular dynamic SIMS imaging of boron-10 and boron-11 isotopes in the same cell delivered by two combined BNCT compounds: *in vitro* studies on human glioblastoma T98G cells. Submitted for publication.

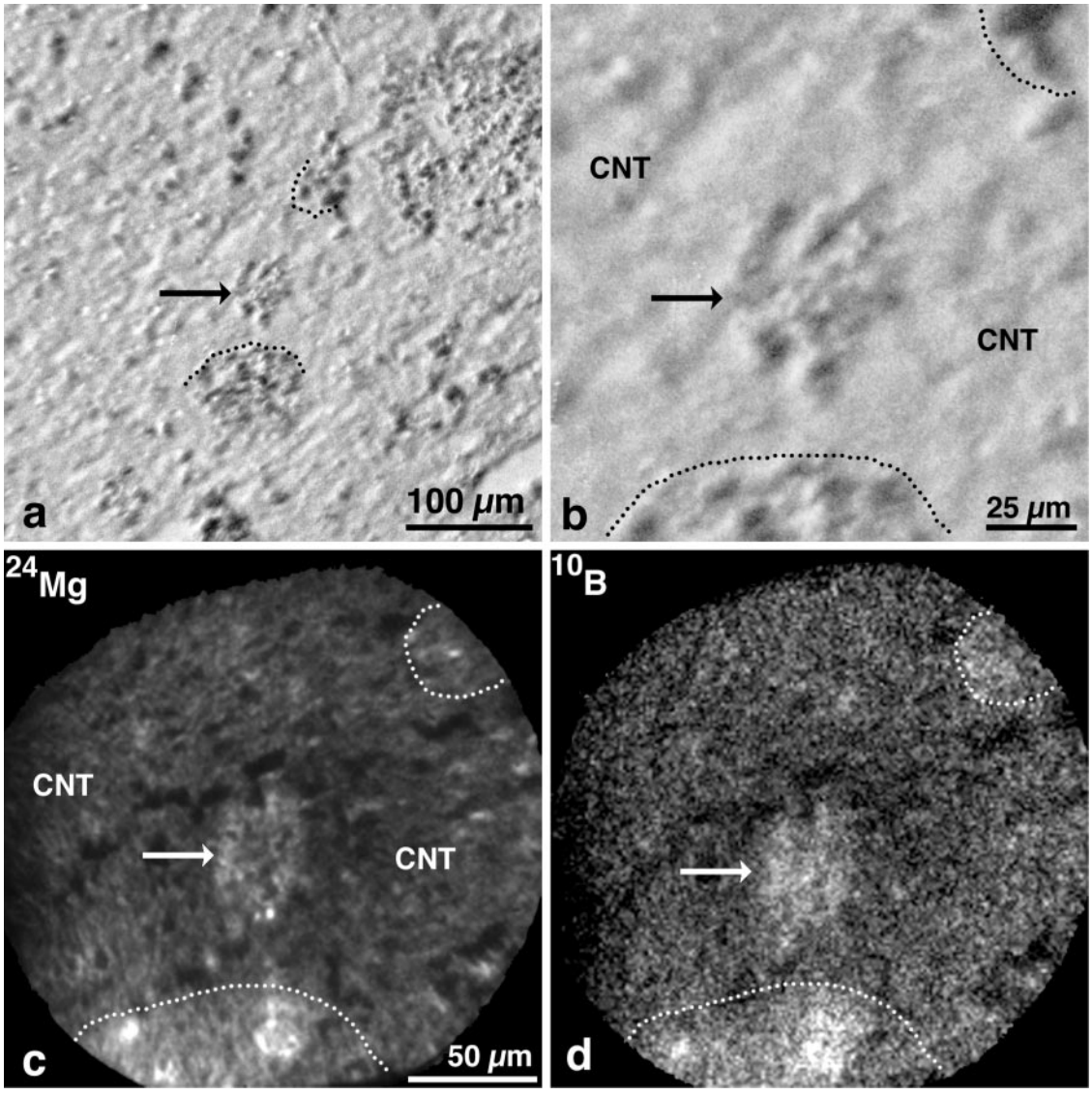

Fig. 2. ^{24}Mg and ^{10}B distribution in clusters of infiltrating tumor cells in the normal brain of a male Fischer 344 rat bearing the 9L gliosarcoma. Adjacent 4-μm thick cryosections were used for optical microscopic and ion microscopic imaging. *a*, optical image of a H&E-stained cryosection on glass. *b*, magnified view of the central part of *a*. *c* and *d*, ion images of ^{24}Mg and ^{10}B, respectively, from the same region of analysis on the freeze-dried cryosection. *Arrows* in *a–d*, cluster of 7–8 infiltrating tumor cells. ···· in *a–d* outline part of the edges of clusters of infiltrating tumor cells showing significantly higher levels of ^{24}Mg (*c*) and ^{10}B (*d*) than the CNT. Scale for *d* is shown in *c*.

cellular outlines are ill defined. The black arrow in Fig. 1*a* indicates a region of tissue with spongiform circular spaces, signs of vasogenic edema, which are often evident along the tumor-brain interface. In Fig. 1*a*, the portion of the CNT above the interface appears to have minimal tumor cell infiltration. The optical image correlates with the region on an adjacent cryosection of tissue analyzed by ion microscopy (Fig. 1, *b–f*). The change of brightness of the ion image shown in Fig. 1*b* reflects the gradient of ^{10}B concentration across the interface (dotted line) between the MTM and the CNT. These observations indicate that ^{10}B from BPA accumulates in the MTM in higher concentration than that observed in the CNT. This pattern of ^{10}B distribution may be attributable in part to enhanced delivery of BPA through the damaged BBB associated with the growth of the MTM. The elevated level of ^{10}B in the MTM is also associated with a higher specificity of BPA for tumor cells (see "Discussion").

Fig. 1 also includes ion images taken of ^{24}Mg, ^{39}K, ^{23}Na, and ^{40}Ca (Fig. 1, *c–f*, respectively) from the same region of analysis as shown in the ^{10}B ion image. The ^{24}Mg distribution shown in Fig. 1*c* is representative for all of the tissues studied, including those from the F98 rat glioma, and the estimated concentration of ^{24}Mg in the MTM was higher than that estimated in the CNT. Clusters[6] of tumor cells infiltrating the normal brain showed this same pattern of Mg distribution (see Figs. 2 and 3). Furthermore, we have made observations of these same elevated levels of ^{24}Mg in the MTM and clusters of infiltrating tumor cells in rats not treated with BPA. The pattern of distribution of Mg in the MTM, clusters of tumor cells infiltrating the normal brain, and in the CNT is an important marker of these histological features that facilitates identification when using ion microscopy.[7] What is evident in the ^{24}Mg image (Fig. 1*c*) is a region of diminished brightness just above the dotted line showing the position of tumor-brain interface. This area corresponds to a portion of the CNT affected by

[6] In this paper the term cluster denotes cross-sections of infiltrating tumor cells in the normal brain and away from the MTM.

[7] D. R. Smith, and S. Chandra, Elevated levels of total magnesium as a marker for brain tumors and infiltrating tumor cells in animal models revealed by SIMS ion microscopy, manuscript in preparation.

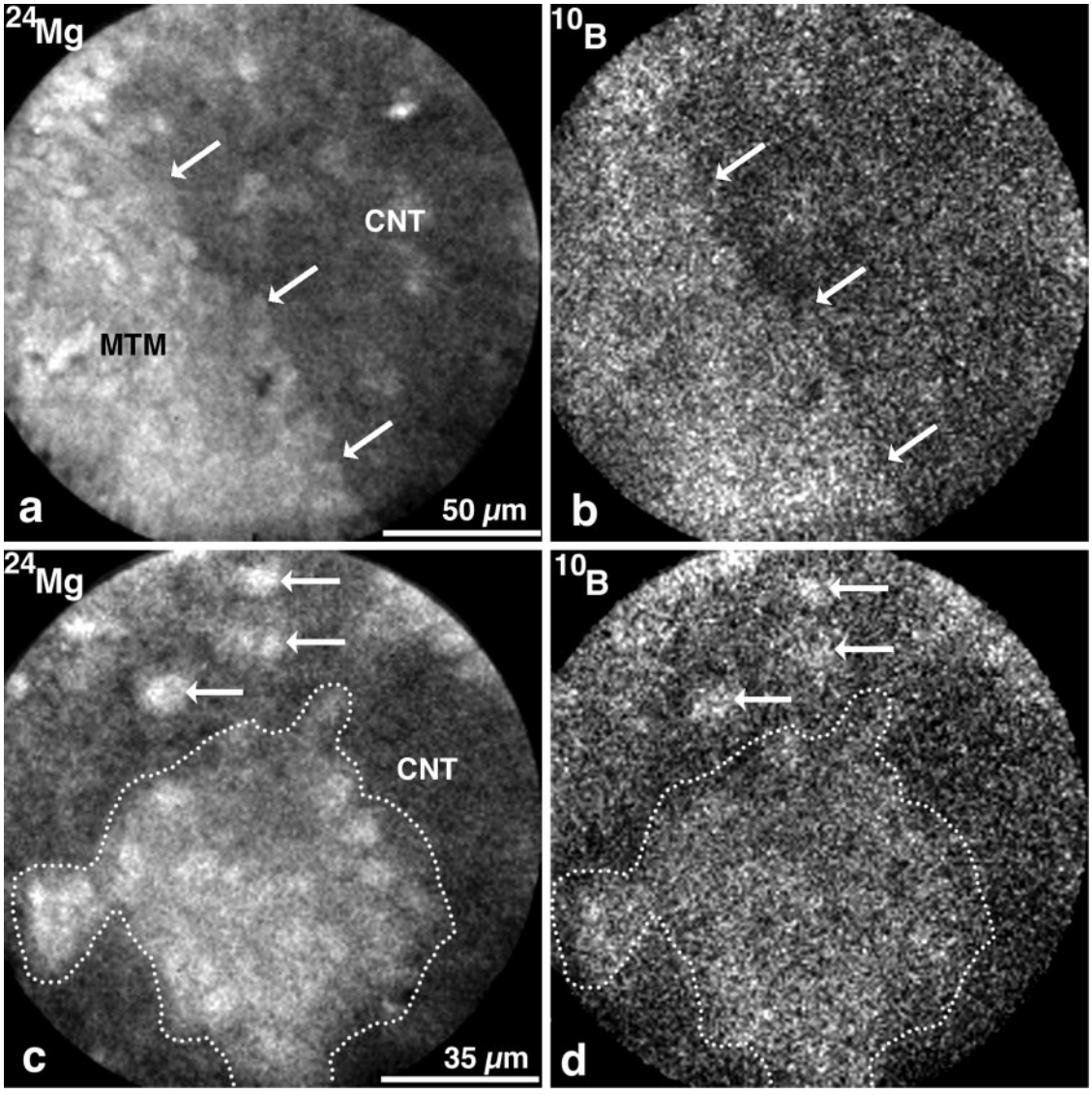

Fig. 3. ^{24}Mg and ^{10}B distribution in the MTM and clusters of tumor cells infiltrating the normal brain of male Fischer 344 rats bearing the F98 glioma. The ion images in *a–d* were acquired from frozen freeze-dried 4-μm thick cryosections from two different rats, respectively. *a* and *b*, ion images of ^{24}Mg and ^{10}B, respectively, from the same region of analysis after i.c. administration of BPA without BBB-D. *c* and *d*, ion images of ^{24}Mg and ^{10}B, respectively, from the same region of analysis after i.c. administration of BPA with BBB-D. *Arrows* in *a* and *b*, interface between a portion of the MTM and the CNT. *Arrows* in *c* and *d*, individual tumor cell nuclei showing significantly higher levels of ^{24}Mg and ^{10}B than the CNT. ···· in *c* and *d* enclose clusters of tumor cells. Note the heterogeneous distribution of ^{24}Mg and ^{10}B in the tumor cell nuclei of *c* and *d*, respectively. Scale for *b* is shown in *a*. Scale for *d* is shown in *c*.

edema (see black arrow in Fig. 1*a*). The more densely packed CNT surrounds the edematous tissue and is evident by the brighter ^{24}Mg signal in the top portion of Fig. 1*c*. No appreciable gradients of ^{39}K and ^{23}Na were observed between the MTM and the CNT (Fig. 1, *d* and *e*). ^{39}K/^{23}Na ratios, indicators of the cryogenic preservation of the *in vivo* distribution of ^{10}B, were satisfactory with values ranging from 3/1 to 8/1. The distribution of ^{10}B was similar among replicate samples and did not correlate with the range of ^{39}K/^{23}Na ratios. The distribution of ^{40}Ca shown in Fig. 1*f* is opposite of that observed for ^{10}B (Fig. 1*b*) and ^{24}Mg (Fig. 1*c*). The edematous CNT shown in the ^{24}Mg ion image (Fig. 1*c*) is also evident in ^{40}Ca image and shows approximately the same intensity as that observed for the MTM. Overall, there was no excess accumulation of calcium in the MTM or the CNT to indicate that any gross damage had occurred to the tissue during preparation (20). The pattern of distribution of ^{12}C (image not shown), was similar to that shown in the images of ^{39}K and ^{23}Na (Fig. 1, *d* and *e*), with no appreciable gradient between the MTM and the CNT. The patterns of distribution of these analytes are strong indicators that SIMS matrix effects[8] are minimal and that the *in vivo* distribution of ^{10}B has been preserved.

The 9L gliosarcoma as well as the F98 glioma exhibit microscopic infiltrative patterns similar to that in human brain tumors. Fig. 2*a* shows a representative optical image of a cryosection stained with H&E from a rat bearing the 9L gliosarcoma after receiving BPA. Fig. 2*b* is a magnified view of the central part of Fig. 2*a*. The ion images of ^{24}Mg (Fig. 2*c*) and ^{10}B (Fig. 2*d*) were acquired from a freeze-dried cryosection of tissue adjacent to that in the optical image. The arrows in Fig. 2, *a–d* indicate a cluster of 7–8 infiltrating tumor cells. The dotted lines directly below this outlines the edge of a larger cluster. The dotted line above the arrow in Fig. 2*a* and in the upper right quadrants of Fig. 2, *b–d* outlines part of the edge of a small cluster of

[8] "SIMS matrix effects" is a general term used to describe the alteration of the signal of an analyte by the surrounding chemical, compositional, and structural environment. Chandra *et al.* (19) provide an in-depth discussion of these effects in biological specimens.

Table 1 *Comparison of ^{10}B concentrations in the MTM, clusters of infiltrating tumor cells, and contiguous normal brain tissues of the 9L rat gliosarcoma and F98 rat glioma after treatment with BPA*

Male Fischer 344 rats bearing the 9L gliosarcoma were administered BPA as a fructose complex in a single i.p. injection. Four rats (trial 1) received 1200 mg BPA/kg b.w. Eight rats (trial 2) received 600 mg BPA/kg b.w. The results of the ion microscopy analyses of tissues from trials 1 and 2 were combined, because observations revealed a similar pattern of boron uptake. Four male Fischer 344 rats bearing the F98 glioma were administered 300 mg BPA/kg b.w. in a fructose complex via a single i.c. injection. Two of these rats were infused with mannitol to induce osmotic BBB-D. The remaining two rats were infused with saline as controls.

Tumor model	BBB-D (yes/no)	$[^{10}B]_{MTM}$ (μg/g)[a]	$[^{10}B]_{clusters}$ (μg/g)[a]	$[^{10}B]_{CNT}$ (μg/g)[a]	$[^{10}B]_{tumor}$:$[^{10}B]_{CNT}$[b]	$[^{10}B]_{MTM}$:$[^{10}B]_{clusters}$[b]
9L	no	99 ± 36		27 ± 12	3.7 ± 2.1	
9L	no		47 ± 15	16 ± 8	2.9 ± 1.7	2.1 ± 1.0
F98	no	26 ± 6		9 ± 4	2.9 ± 1.4	
F98	no		13 ± 4	6 ± 3	2.2 ± 1.3	2.0 ± 0.8
F98	yes	49 ± 10		9 ± 4	5.4 ± 2.6	
F98	yes		21 ± 7	7 ± 2	3.0 ± 1.3	2.3 ± 0.9

[a] Concentrations are given as wet weight values in μg ^{10}B/g (ppm) tissue assuming 85% cell water content (mean ± SD).
[b] Calculated as the ratio of the means.

infiltrating tumor cells. In the upper right quadrant of Fig. 2*a*, the dark-stained nuclei of tumor cells are discernible in the cross-section of a relatively large cluster. In Fig. 2*c*, the pattern of distribution of ^{24}Mg highlights the tumor cells in the darker background of the CNT. In Fig. 2*d*, the regions identified as clusters also have a brighter ^{10}B signal than regions identified as the CNT. Quantitatively, this indicates that clusters of infiltrating tumor cells accumulate higher concentrations of ^{10}B from BPA relative to that in the CNT.

Fig. 3 shows ion images of ^{24}Mg and ^{10}B from rats bearing the F98 glioma after receiving BPA by i.c. injection without (Fig. 3, *a* and *b*) or with BBB-D (Fig. 3, *c* and *d*). In Fig. 3*a*, arrows indicate a portion of an interface between the MTM and the CNT. The morphology of the F98 rat glioma is similar to the 9L gliosarcoma and is revealed in the ^{24}Mg ion image. The MTM shows densely packed nuclei with ill-defined cellular outlines. The corresponding ^{10}B ion image shown in Fig. 3*b* shows brighter signals arising from the MTM indicating higher boron concentrations relative to that estimated for the CNT. In Fig. 3*c*, the arrows indicate regions of high ^{24}Mg intensity from cross-sections of individual cell nuclei. These same regions are indicated by arrows in the corresponding ion image of ^{10}B (Fig. 3*d*). Close examination of cell nuclei reveals a heterogeneous distribution of ^{24}Mg and ^{10}B, similar to that observed for the 9L gliosarcoma (see Fig. 2, *c* and *d*). A dotted line in Fig. 3*c* encloses a large cluster of infiltrating tumor cells in which individual cell nuclei are clearly discernible. In Fig. 3*d*, this same region shows similar image intensity to the individual cell nuclei indicated with arrows. The CNT is lower in intensity and subsequently has lower concentrations of ^{10}B than in the clusters of infiltrating tumor cells.

The estimated ^{10}B concentrations in the MTM, clusters of infiltrating tumor cells, and the CNT of the 9L gliosarcoma and the F98 glioma rat brain tumor models treated with BPA are shown in Table 1. Considering the data from the two rat brain tumor models, the ratio of ^{10}B in the MTM or clusters to the CNT ($[^{10}B]_{tumor}$:$[^{10}B]_{CNT}$) ranged from 2.2:1 to 5.4:1. BBB-D in the F98 glioma model resulted in a substantial increase in the ^{10}B concentrations in the tumor tissues, 49 *versus* 26 μg/g in the MTM and 21 *versus* 13 μg/g in the clusters. The concentration of ^{10}B within the CNT of the F98 glioma model, with and without BBB-D, essentially remained unchanged.

Table 1 also shows the MTM:cluster ^{10}B concentration ratio ($[^{10}B]_{MTM}$:$[^{10}B]_{clusters}$) for the 9L gliosarcoma and the F98 glioma rat brain tumor models. A consistent pattern was evident in the two animal models and the multiple routes of delivery of BPA. The ^{10}B concentration in the MTM was essentially twice that observed in the clusters of tumor cells infiltrating the normal brain.

Continuous Timed i.v. Infusions: BPA and the Rat 9L Gliosarcoma. Three pairs of rats with the 9L gliosarcoma received BPA in a continuous timed i.v. infusion over 2, 3, and 6 h, respectively, and a fourth rat was infused for 24 h. The results of the ion microscopy analyses of cryogenically prepared tissues from these four sets of rats are shown in Table 2. The ratio of the concentration of ^{10}B in the MTM to that in the clusters is the highest (2.7:1) for the 2-h infusion. The ratio decreases to 2.0:1 for the 3-h infusion. After 6 h, the ratio is 1.4:1, and the concentration of ^{10}B in the clusters has nearly doubled that observed for the 2- and 3-h infusions. For the 24-h infusion, the ratio approached unity. The concentration of ^{10}B in the normal brain was similar for the four infusions [20 ± 8, 24 ± 6, 18 ± 2, and 24 ± 3 μg/g (mean ± SD) for 2, 3, 6, and 24 h, respectively].

DISCUSSION

The spatial resolution of the CAMECA IMS-3f ion microscope is comparable with a high-quality light microscope. This, in combination with the relatively wide field-of-view (150-μm diameter) enables the boron distribution in multiple histological features to be measured in a single image. The representative ion microscopy images of ^{10}B from the BPA treated rat brain tissues (Figs. 1–3) revealed a distinct change in brightness at the interface between the MTM and CNT and the clusters of infiltrating tumor cells and the CNT, respectively. The brightness of the ^{10}B ion images was directly proportional to the analyte concentration within a region defined by the spatial resolution of the ion microscope. The differential accumulation of ^{10}B between

Table 2 *BPA ^{10}B concentrations in the 9L gliosarcoma MTM and clusters of tumor cells infiltrating the normal rat brain 1 h after i.v. infusion*

Three pairs of male Fischer 344 rats bearing the 9L gliosarcoma were administered BPA as a fructose complex for 2, 3, and 6 h, respectively. A dose rate of 250 mg BPA/kg/h resulted in blood-volume overload and was lethal for rats infused for 24 h. Only one rat survived even when the dose rate was reduced to 125 mg BPA/kg/h. The concentration of ^{10}B in the normal brain was similar for the four infusion times [20 ± 8, 24 ± 6, 18 ± 2, and 24 ± 3 (mean ± SD) for 2, 3, 6, and 24 h, respectively].

Dose rate (mg BPA/kg/h)	Infusion time (h)	$[^{10}B]_{MTM}$ (μg/g)[a]	$Range_{MTM}$ (μg/g)[a]	$[^{10}B]_{clusters}$ (μg/g)[a]	$Range_{clusters}$ (μg/g)[a]	$[^{10}B]_{MTM}$:$[^{10}B]_{clusters}$[b]
250	2	83 ± 23	36–170	31 ± 12	14–62	2.7 ± 1.3
250	3	75 ± 30	31–135	37 ± 7	24–52	2.0 ± 0.9
250	6	90 ± 14	63–124	65 ± 11	51–83	1.4 ± 0.3
125	24	53 ± 10	41–73	52 ± 14	34–81	1.0 ± 0.3

[a] Concentrations are given as wet weight values in μg ^{10}B/g (ppm) assuming 85% cell water content (mean ± SD).
[b] Calculated as the ratio of the means.

the MTM and the CNT by itself was not an indicator of the specificity of BPA for the tumor cells, because compound delivery to the MTM is enhanced by a compromised BBB. However, the differential accumulation of ^{10}B between clusters of infiltrating tumor cells and the CNT provided direct visual confirmation of the specificity of BPA in tumor cells. Clusters of infiltrating tumor cells outside the MTM, where the mode of compound delivery takes place across an intact BBB, are exposed to the same extracellular source of BPA as the normal brain with little or no contribution from the blood supply of the MTM. A recent study (33) using cultured 9L gliosarcoma cells supports the hypothesis that BPA is actively transported through the cell membrane by the L amino acid transport system, and the selectivity of the compound is increased in malignant cells.

From ion images of ^{10}B distributions we were able to calculate the T:Br ^{10}B concentration ratio ($[^{10}B]_{tumor}$:$[^{10}B]_{CNT}$ in Table 1). This ratio is particularly important because the effectiveness of BNCT is related primarily to the selective accumulation of the boron delivery agent in the tumor relative to the CNT. As determined by ion microscopy, the T:Br ^{10}B concentration ratio for the MTM of the 9L gliosarcoma rat brain tumor model after i.p. injection of BPA was ~3.7:1 (Table 1) compared with ~3.5:1 for the T:Br and T:Bl[9] boron concentration ratios from identically treated rats (21). In another study using the 9L gliosarcoma (25), the effect of increasing the i.v. infusion time at a constant dose rate or increasing the dose rate at a fixed i.v. infusion time resulted in higher absolute boron concentrations in both tumor and blood, yet the T:Bl ratios remained essentially unchanged (3.0:1 to 4.0:1). Patients treated in the Phase I/II clinical trials at Brookhaven National Laboratory were found to have similar "fixed" T:Br and T:Bl boron concentration ratios (~3.5:1) after administration of a 2-h i.v. infusion of varying doses of BPA (34).

The observation of small, fixed T:Br and T:Bl boron concentration ratios for BPA is not a negative factor for the use of this compound as a boron delivery agent for BNCT. As shown in Tables 1 and 2, relatively high concentrations of ^{10}B can be delivered to the MTM of the rat brain tumor models. Similar high levels of ^{10}B have been determined in the analysis of gross tumor specimens from patients given a 2-h i.v. BPA infusion (34). This is important because dosimetric calculations, assuming a fixed T:Bl boron concentration ratio of 3:1, indicate that the therapeutic ratio (tumor radiation dose to the normal tissue radiation dose) of BNCT improves as more boron compound is administered and higher absolute ^{10}B concentrations are produced in both the tumor and normal tissues (8). This can be attributed to the threshold for effective BNCT, which is estimated to be 10^9 ^{10}B atoms distributed uniformly throughout a tumor cell (7). The threshold corresponds to the minimum value of boron concentration (approximately 15–30 μg ^{10}B/g), which sufficiently raises the BNC-radiation dose to the tumor above that of the nonspecific background dose associated with the neutron beam alone. It is more important to have higher ^{10}B levels in the tumor at a fixed T:Br ratio than lesser amounts of ^{10}B in the tumor (below the threshold) but very high T:Br ratios (8, 21). This is because of the background radiation dose attributable to capture reactions with normal tissue ^{1}H and ^{14}N. A review of BNCT radiobiology can be found in a recent publication (8).

In the present study, rats bearing the F98 glioma were administered BPA by i.c. injection with and without BBB-D. Hyperosmotic mannitol-induced BBB-D followed by i.c. delivery is one strategy being explored (6) to optimize the delivery of ^{10}B to brain tumors and to tumor cells in regions protected by the BBB. BBB-D transiently and reversibly increases the permeability of capillaries in both the tumor and the normal brain. For agents such as BPA, which exhibit rapid blood clearance, moderate lipophilicity, and low neurotoxicity, the i.c. route of delivery is more effective for targeting brain tumors than i.v. delivery. It has been shown (35) that i.c. injection of BPA in rats with the F98 glioma results in T:Bl boron concentration ratios more than double that after i.v. delivery. In a similar study (28) mannitol-induced BBB-D followed by a 3-min i.c. injection of BPA was shown to enhance the T:Br ^{10}B concentration ratio relative to i.c. delivery without BBB-D. In that same study, average T:Br and T:Bl concentration ratios of 5.2:1 and 5.6:1, respectively, were observed 2.5 h after BBB-D and compound administration. Without BBB-D, the corresponding T:Br and T:Bl ratios were 4.3:1 and 4.1:1, respectively. For identically treated rats, the ion microscopy derived T:Br boron concentration ratios determined for the MTM of the F98 glioma with and without BBB-D, were 5.4:1 and 2.9:1, respectively ($[^{10}B]_{tumor}$:$[^{10}B]_{CNT}$ in Table 1). In previous studies (35), the effectiveness of BBB-D and i.c. compound delivery for targeting tumor cells invading normal brain at some distance away from the MTM was unknown. The results in Table 1 provide the first direct evidence of the effect of BBB-D on BPA-mediated ^{10}B delivery to clusters of tumor cells invading normal brain. The concentration of ^{10}B was found to increase significantly ($P < 0.05$), ~60% after BBB-D. This resulted in a higher T:Br boron concentration ratio ($[^{10}B]_{tumor}$:$[^{10}B]_{CNT}$ in Table 1), which increased from 2.2:1 (without BBB-D) to 3.0:1 (with BBB-D), with no appreciable difference in the normal brain boron concentrations for either treatment. Dosimetric calculations (36) indicate that the increase in the T:Br ^{10}B concentration ratios observed after BBB-D and i.c. injection of BPA could result in an increase in the therapeutic ratio exceeding 25%.

A direct comparison of the experimental results shown in Table 1 for the 9L gliosarcoma with those of the F98 glioma was complicated by the number of different treatment variables (*i.e.*, i.p. injection, i.c. injection, compound doses, tissue boron clearance times, with and without BBB-D). However, these variables were normalized by calculating a MTM:cluster ^{10}B concentration ratio ($[^{10}B]_{MTM}$:$[^{10}B]_{clusters}$) for each treatment. Examination of the last column of Table 1 reveals a consistent pattern of ^{10}B distribution. The ^{10}B concentration in the MTM is at least twice that of the clusters of tumor cells invading the normal brain. This information has important implications for the success of BNCT, because clusters and individual tumor cells infiltrating the normal brain are potential sites of post-therapy tumor recurrence. In the Phase I/II clinical trials of BNCT at Brookhaven National Laboratory, BPA was administered to patients in a continuous 2-h i.v. infusion. The question arises as to whether this length of time was sufficient for BPA to concentrate in infiltrating tumor cells and produce tumor:cluster boron concentration ratios better (lower) than those observed in the present study. To address this, BPA was administered to rats bearing the 9L gliosarcoma in a study to simulate the continuous 2-h i.v. infusion schedule used (4) for the treatment of patients in the Brookhaven clinical trials. The observations from this study are shown in the first row of Table 2. After a 2-h i.v. infusion, the MTM:cluster ^{10}B concentration ratio ($[^{10}B]_{MTM}$:$[^{10}B]_{clusters}$) was 2.7:1, slightly higher and essentially worse than the ratios shown in Table 1. Furthermore, a wide range of ^{10}B concentrations (36 μg/g-170 μg/g) were observed in the MTM. The latter also may increase the likelihood of post-therapy tumor recurrence. Indeed, it has been suggested (4) that the absence of long-term tumor control in patients receiving relatively high minimal tumor volume doses (40–55 Gy-Eq) may have been attributable to a nonuniform distribution of ^{10}B in tumor cells after a single 2-h i.v. infusion.

In the Brookhaven clinical trials, the radiation dose to the tumor was estimated from blood-boron concentrations determined at the

[9] After treatment with BPA, the average concentration of boron in the normal brain is approximately equal to or slightly less than that in blood for both experimental animals and humans (8).

time of BNCT. This is possible, because it has been shown (34) that the amount of boron in the blood is a linear function of the BPA dose and the tumor tissue boron concentration is a linear function of the density of viable-appearing tumor cells. This correlation was used to establish the fixed T:Bl concentration ratio (~3.5:1) for BPA in patients and was assumed to be valid not only for tumor cells in the MTM but for tumor cells infiltrating normal brain within the irradiated target volume (4). Our observations using ion microscopy strongly suggest that the fixed T:Bl[9] boron concentration ratio of 3.5:1 is an overestimate for tumor cells infiltrating normal brain (see Tables 1 and 2). The boron concentration in infiltrating tumor cells was most likely lower than that determined for the MTM and may have been a contributing factor in the lack of correlation between the BNCT radiation doses and the time-to-tumor progression in those patients treated at the Brookhaven National Laboratory. It would have been impossible to determine the *in vivo* boron concentration in zones of infiltrating tumor cells from patients who underwent BNCT, because this would have required additional biopsies at varying distances from the resection cavity at the time of BNCT.

The i.v. infusion study using rats bearing the 9L gliosarcoma to model the conditions of BPA administration to patients was extended from 2 h to include continuous 3-, 6-, and 24-h infusions. This was performed to determine whether it was possible to improve the MTM:cluster ^{10}B concentration ratio after administration of BPA and still maintain the relatively low concentrations of ^{10}B in the normal brain that were observed 1 h after the 2-h infusion. The results are shown in Table 2. The 2-h infusion resulted in the highest ^{10}B concentration ratio (2.7:1). However, inspection of the estimated concentrations of ^{10}B with their respective ranges in the MTM and the clusters (Table 2) indicates that the 2- and 3-h infusions were not statistically different from each other. After the 6-h infusion, the estimated ^{10}B content in clusters of tumor cells infiltrating the normal brain changed significantly ($P < 0.05$), with an ~90% increase relative to the 2- and 3-h infusions. This improved the MTM:cluster ^{10}B concentration ratio (1.4:1), because there was only a slight increase in the ^{10}B level of the MTM. The 24-h infusion[10] resulted in a ratio of unity. The ^{10}B concentration in the normal brain was constant and low throughout the study and, most importantly, independent of the length of infusion time [20 ± 8, 24 ± 6, 18 ± 2, and 24 ± 3 μg/g (mean ± SD) for 2, 3, 6, and 24 h, respectively]. These observations are significant, because they show for the first time that it is possible to enhance BPA-mediated ^{10}B delivery to infiltrating tumor cells in the normal brain by increasing the duration of the i.v. infusion. Subsequently, it may be possible to deliver substantially greater doses of BNC-radiation to tumor cells away from the blood supply of the MTM.

BPA is delivered to the MTM through the tumor blood supply in which the BBB is compromised. Infiltrating tumor cells away from the blood supply of the MTM receive BPA, which is actively transported across an intact BBB but passively diffuses through interstitial fluids. The data in Table 2 are consistent with these two different modes of compound delivery. The 2- and 3-h infusions are not of sufficient length for BPA to establish equilibrium in infiltrating tumor cells. Only after a 6-h infusion did we observe a significant change in the concentration of ^{10}B in the clusters of tumor cells invading the normal brain. The estimated ^{10}B concentrations in the MTM for the 2-, 3-, and 6-h infusions suggests that the tumor cell uptake of BPA in the MTM is in equilibrium with the boron content of extracellular fluids. This is supported by the data for the 24-h infusion. When the dose rate was decreased by 50%, the observed ^{10}B concentration in the MTM decreased accordingly (~40% relative to the 6-h infusion).

[10] The 24-h i.v. infusion of BPA is practical in animal studies only.

Both the 9L rat gliosarcoma and the F98 rat glioma have an infiltrative pattern of growth similar to human brain tumors. After treatment with BPA, the rat models exhibited T:Br ^{10}B concentration ratios for the MTM comparable with those found in patients treated in clinical trials. With ion microscopy we were able to show that with different modes of BPA administration, infiltrating tumor cells had significantly lower ^{10}B levels relative to that observed in the MTM. However, the delivery of BPA to infiltrating tumor cells was enhanced by extending the duration of the i.v. infusion from 2 h to 6 h. Additional support for a 6-h infusion is provided by other ion microscopy studies[5,11] exploring the kinetics of boron uptake in the T98G human glioblastoma cell line. In those studies, the intracellular ^{10}B concentration more than doubled for cells exposed to BPA for 6 h relative to cells exposed for 1 h. Indeed, the observations made here as well as those on the T98G human glioblastoma cell line[5,11] have provided the foundation for new clinical trials of BNCT in Sweden, where the 6-h infusion protocol for BPA administration is currently being evaluated[12] for the treatment of glioblastoma multiforme.

ACKNOWLEDGMENTS

We thank P. L. Micca (Medical Department, Brookhaven National Laboratory, Upton, NY), M. M. Nawrocky (Medical Department, Brookhaven National Laboratory, Upton, NY), and J. H. Rotaru (Department of Pathology, The Ohio State University, Columbus, OH) for technical assistance; and A. D. Chanana and D. N. Slatkin (Medical Department, Brookhaven National Laboratory, Upton, NY) for their helpful comments throughout these studies.

REFERENCES

1. Hatanaka, H., and Nakagawa, Y. Clinical results of long-surviving brain tumor patients who underwent boron neutron capture therapy. Int. J. Radiat. Oncol. Biol. Phys., *28:* 1061–1066, 1994.
2. Gabel, D., Preusse, D., Haritz, D., Grochulla, F., Haselsberger, K., Frankhauser, H., Ceberg, C., Peters, H-D., and Klotz, U. Pharmacokinetics of $Na_2B_{12}H_{11}SH$ (BSH) in patients with malignant brain tumors as prerequisite for a Phase I clinical trial of boron neutron capture therapy. Acta Neurochir., *139:* 606–612, 1997.
3. Nakagawa, Y., and Hatanaka, H. Boron neutron capture therapy: clinical brain tumor studies. J. Neuro-Oncol., *33:* 105–115, 1997.
4. Chanana, A. D., Capala, J., Chadha, M., Coderre, J. A., Diaz, A. Z., Elowitz, E. H., Iwai, J., Joel, D. D., Liu, H. B., Ma, R., Pendzick, N., Peress, N. S., Shady, M. S., Slatkin, D. N., Tyson, G. W., and Wielopolski, L. Boron neutron capture therapy for glioblastoma multiforme: interim results from the phase I/II dose-escalation studies. Neurosurgery (Baltimore), *44:* 1182–1193, 1999.
5. Hall, E. J. Radiobiology for the Radiologist, 5th Ed. pp. 73–74. Philadelphia, PA: J. B. Lippincott Company, 2000.
6. Barth, R. F., Soloway, A. H., Goodman, J. H., Gahbauer, R. A., Gupta, N., Blue, T. E., Yang, W., and Tjarks, W. Boron neutron capture therapy of brain tumors: an emerging therapeutic modality. Neurosurgery (Baltimore), *44:* 433–451, 1999.
7. Fairchild, R. G., and Bond, V. P. Current status of ^{10}B boron neutron capture therapy: enhancement of tumor dose via beam filtration and dose rate, and the effects of these parameters on minimum boron content: a theoretical evaluation. Int. J. Radiat. Oncol. Biol. Phys., *11:* 831–840, 1985.
8. Coderre, J. A., and Morris, G. M. The radiation biology of boron neutron capture therapy. Radiat. Res., *151:* 1–18, 1999.
9. Probst, T. U. Methods for boron analysis in boron neutron capture therapy (BNCT). A review. Fresenius' J. Anal. Chem., *364:* 391–403, 1999.
10. Sah, R. N., and Brown, P. H. Boron determination—a review of analytical methods. Microchem. J., *56:* 285–304, 1997.
11. Fairchild, R. G., Gabel, D., Laster, B. H., Greenberg, D., Kiszenick, W., and Micca, P. L. Microanalytical techniques for boron analysis using the ^{10}B(n, α)^{7}Li reaction. Med. Phys., *13:* 50–56, 1986.
12. Barth, R. F., Adams, D. M., Soloway, A. H., Mechetner, E. B., Alam, F., and Anisuzzaman, A. K. M. Determination of boron in tissues and cells using direct-current plasma atomic emission spectroscopy. Anal. Chem., *63:* 890–893, 1991.
13. Johnson, D. A., Siemer, D. D., and Bauer, W. F. Determination of nanogram levels of boron in milligram-sized tissue samples by inductively coupled plasma-atomic emission spectroscopy. Anal. Chim. Acta, *270:* 223–230, 1992.
14. Castaing, R., and Slodzian, G. Microanalyse par émission ionique secondaire. J. Microsc. (Paris), *1:* 395–410, 1962.

[11] S. Chandra, D. R. Lorey, II, and D. R. Smith, unpublished observations.

[12] Jacek Capala, Manager, Medical Physics and NCT Research, Studsvik Medical, personal communication.

15. Smith, D. R., Chandra, S., Coderre, J. A., and Morrison, G. H. Ion microscopy imaging of ^{10}B from *p*-boronophenylalanine in a brain tumor model for boron neutron capture therapy. Cancer Res., *56:* 4302–4306, 1996.
16. Morris, G. M., Smith, D. R., Patel, H., Chandra, S., Morrison, G. H., Hopewell, J. W., Rezvani, M., Micca, P. L., and Coderre, J. A. Boron microlocalization in oral mucosal tissue: implications for boron neutron capture therapy. Br. J. Cancer, *82:* 1764–1771, 2000.
17. Chandra, S., Smith, D. R., and Morrison, G. H. Subcellular imaging by dynamic SIMS ion microscopy. Anal. Chem., *72:* 104A–114A, 2000.
18. Galle, P., Francoise, E., Fabienne, D., and Lili, Z. Mapping the subcellular distribution of biomolecules at the ultrastructural level by ion microscopy. Cell. Mol. Biol., *42:* 325–334, 1996.
19. Chandra, S., Ausserer, W. A., and Morrison, G. H. Evaluation of matrix effects in ion microscopic analysis of freeze-fractured, freeze-dried cultured cells. J. Microsc. (Oxf.), *148:* 223–239, 1987.
20. Chandra, S., and Morrison, G. H., Sample preparation of animal tissues and cell cultures for secondary ion mass spectrometry (SIMS) microscopy. Biol. Cell, *74:* 31–42, 1992.
21. Coderre, J. A., Button, T. M., Micca, P. L., Fisher, C., Nawrocky, M. M., and Liu, H. B. Neutron capture therapy of the 9L gliosarcoma using the *p*-boronophenylalanine-fructose complex. Int. J. Radiat. Oncol. Biol. Phys., *30:* 643–652, 1994.
22. Yoshino, K., Suzuki, A., Mori, Y., Kanihana, H., Honda, C., Mishima, Y., Kobayashi, T., and Kanda, K. Improvement of solubility of *p*-boronophenylalanine by complex formation with monosaccharides. Strahlenther. Onkol., *165:* 127–129, 1989.
23. Joel, D. D., Fairchild, R. G., Laissue, J. A., Saraf, S. K., Kalef-Ezra, J. A., and Slatkin, D. N. Boron neutron capture therapy of intracerebral rat gliosarcomas. Proc. Natl. Acad. Sci. USA, *87:* 9808–9812, 1990.
24. Barth, R. F. Rat brain tumor models in experimental neuro-oncology: the 9L, C6, T9, F98, RG2 (D74), RT-2 and CNS-1 gliomas. J. Neuro-Oncol., *36:* 91–102, 1998.
25. Joel, D. D., Coderre, J. A., Micca, P. L., and Nawrocky, M. M. Effect of dose and infusion time on the delivery of *p*-boronophenylalanine for neutron capture therapy. J. Neuro-Oncol., *41:* 213–221, 1999.
26. Ko, L., Koestner, A., and Wechsler, W. Morphological characterization of nitrosourea-induced glioma cell lines and clones. Acta Neuropathol., *51:* 23–31, 1980.
27. Clendenon, N. R., Barth, R. F., Gordon, W. A., Goodman, J. H., Alam, F., Staubus, A. E., Boesel, C. P., Yates, A. J., Moeschberger, M. L., Fairchild, R. G., and Kalef-Ezra, J. A. Boron neutron capture therapy of a rat glioma. Neurosurgery, *26:* 47–55, 1990.
28. Yang, W., Barth, R. F., Carpenter, D. E., Moeschberger, M. L., and Goodman, J. H. Enhanced delivery of boronophenylalanine for neutron capture therapy by means of intracarotid injection and blood-brain barrier disruption. Neurosurgery (Baltimore), *38:* 985–992, 1996.
29. Sod, E. W., Crooker, A. R., and Morrison, G. H. Biological cryosection preparation and practical ion yield evaluation for ion microscopic analysis. J. Microsc. (Oxf.), *160:* 55–65, 1989.
30. Ausserer, W. A., Ling, Y-C., Chandra, S., and Morrison, G. H. Quantitative imaging of boron, calcium, magnesium, potassium, and sodium distributions in cultured cells with ion microscopy. Anal. Chem., *61:* 2690–2695, 1989.
31. Smith, D. R., Chandra, S., Coderre, J. A., Barth, R. F., Yang, W., Liu, L., Wilson, J. L., Micca, P. L., Nawrocky, M. M., Rotaru, J. H., and Morrison, G. H. Quantitative ion microscopy imaging of boron-10 in rat brain tumor models for BNCT. *In:* B. Larsson, J. Crawford, and R. Weinreich (eds.), Advances in Neutron Capture Therapy. Volume II, Chemistry and Biology, pp. 308–314. Amsterdam: Elsevier, 1997.
32. Smith, D. R., Joel, D. D., Coderre, J. A., Morris, G. M., Chandra, S., Nawrocky, M. M., Micca, P. L., Patel, H., and Morrison, G. H. Ion microscopy imaging of boron in animal tissue sections for neutron capture therapy. *In:* M. F. Hawthorne, K. Shelly, and R. J. Wiersema (eds.), Frontiers in Neutron Capture Therapy, pp. 893–897. New York, NY: Kluwer Academic/Plenum, 2001.
33. Wittig, A., Sauerwein, W. A., and Coderre, J. A. Mechanisms of transport of *p*-borono-phenylalanine through the cell membrane *in vitro*. Radiat. Res., *153:* 173–180, 2000.
34. Coderre, J. A., Chanana, A. D., Joel, D. D., Elowitz, E. H., Micca, P. L., Nawrocky, M. M., Chadha, M., Gebbers, J-O., Shady, M., Peress, N. S., and Slatkin, D. N. Biodistribution of boronophenylalanine in patients with glioblastoma multiforme: boron concentration correlates with tumor cellularity. Radiat. Res., *149:* 163–170, 1998.
35. Barth, R. F., Yang, W., Rotaru, J. H., Moeschberger, M. L., Joel, D. D., Nawrocky, M. M., Goodman, J. H., and Soloway, A. H. Boron neutron capture therapy of brain tumors: enhanced survival following intracarotid injection of either sodium borocaptate or boronophenylalanine with or without blood-brain barrier disruption. Cancer Res., *57:* 1129–1136, 1997.
36. Coderre, J. A. Boron neutron capture therapy. *In:* S. A. Leibel and T. L. Phillips (eds.), Textbook of Radiation Oncology, pp. 1263–1277. Philadelphia, PA: W. B. Saunders, 1998.

Quantitative Imaging and Microlocalization of Boron-10 in Brain Tumors and Infiltrating Tumor Cells by SIMS Ion Microscopy: Relevance to Neutron Capture Therapy

Duane R. Smith, Subhash Chandra, Rolf F. Barth, et al.

Cancer Res 2001;61:8179-8187.